

## Numerical study and examples on singularities of solutions to anisotropic crystalline curvature flows of nonconvex polygonal curves

Chiaki Hirota, Tetsuya Ishiwata and Shigetoshi Yazaki

### Abstract.

We construct explicit solutions of the anisotropic motion of closed polygonal plane curves by a power of crystalline curvature, in the case where the initial curves are nonconvex and the power is less than one: The solutions develop degenerate pinching singularities of a “whisker”-type and a split-type in finite time, and do not become convex polygons. Moreover, in the splitting case, we conjecture degenerate pinching rate from numerical experiments.

### §1. Introduction

In this paper we consider an evolution equation of a closed, simple  $N$ -sided polygonal curve  $\mathcal{P}(t)$  in the plane  $\mathbb{R}^2$ :

$$(1) \quad V_j = a(\theta_j)\text{sign}(H_j)|H_j|^\alpha$$

for  $j = 0, 1, \dots, N - 1$ , where  $V_j$ ,  $H_j$ ,  $\alpha$  and  $a(\theta_j)$  denote an inward normal velocity of the  $j$ -th edge of  $\mathcal{P}(t)$ , a crystalline curvature, a positive parameter and a positive function which describes anisotropy of mobility, respectively. The detailed formulations will be mentioned later. The interface motions of polygonal curves in a certain class are called *crystalline motion* and the motions which is governed by crystalline curvature are called *crystalline curvature flow*. These interface motions were introduced by J.E. Taylor[18] and S. Angenent and M.E. Gurtin[3] (precise history is found in e.g., [1]). They considered the case where an interfacial energy density is not smooth and its Wulff shape is a convex

---

Received October 31, 2005.

Revised February 26, 2006.

Partially supported by Grant-in-Aid for Encouragement of Young Scientists (Ishiwata: No. 15740056; Yazaki: No. 15740073, 17740063).

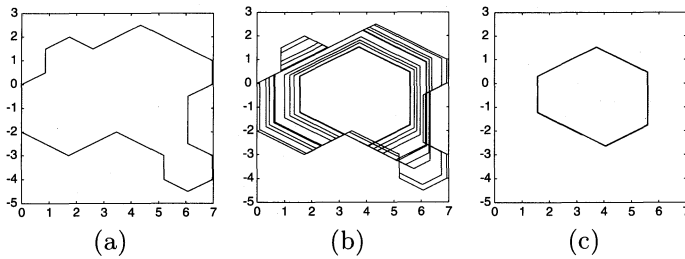


Fig. 1. Numerical simulation for nonconvex solution (case  $\alpha = 1$ ,  $a(\theta_j) \equiv 1$  in (1)): (a) The initial nonconvex curve, (b) Motion of nonconvex solution curve, and (c) The solution curve becomes convex in finite time.

polygon and introduced the suitable class of piecewise linear curve, so-called *admissible curve*, and defined crystalline curvature for admissible curves. Since their pioneer works, various kinds of crystalline motion has been studied by several authors.

For crystalline curvature flow (1), it is known that some kinds of singularities may happen in finite time. When the initial curve  $\mathcal{P}(0)$  is convex, the solution curve shrinks to a single point or collapses to a line segment in finite time. In this case the velocity  $V_j$  and the curvature  $H_j$  diverge to infinity in finite time. We call this phenomena *blow-up*. The blow-up rate and the relation between the blow-up rate and the limit shape are discussed in [2], [11, 15, 16], [17].

If the initial curve  $\mathcal{P}(0)$  is not convex, there is a possibility that self-intersection or admissibility-breaking of solution curves may happen. K. Ishii and H.M. Soner [13] considered the flow  $V_j = H_j$  in the case where the Wulff shape is a regular polygon. They discuss edge-disappearing and non-existence of self-intersection. M.H. Giga and Y. Giga [5] considered a general flow  $V_j = g(\theta_j, H_j)$  and mentioned the *convexity theorem*, which means that nonconvex solution curve becomes convex in finite time (See Fig.1). This type of theorem is shown for smooth curve by curve-shortening flow in [6] and [4]. However, in [14] the examples of nonconvex self-similar solution are shown (see also [12, the second Remark in §3], Example 1 in §3 below and Fig.2). These solutions keep nonconvexity and shrink to a single point. Therefore the convexity theorem does not hold in general. Moreover, L-shaped degenerate pinching is shown in [12] (cf. Example 1): The solution curve keeps nonconvexity and converges to an L-shaped line segment (does not shrink to a single point or collapse to one line segment). That is,

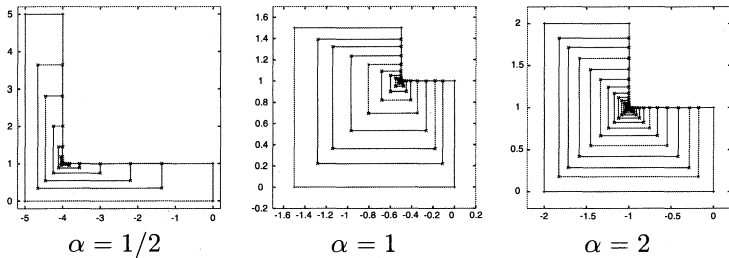


Fig. 2. Nonconvex self-similar solutions: The outermost curve in each figures is the initial curve and the solution curves shrink to a single point.

the motion is more complicated than the convex case. Hence, it is necessary to be clear the conditions for such a convexity theorem holding and for the nonconvexity being preserved. In this short paper, we show some examples of degenerate pinching phenomena and self-intersection of nonconvex curve. Also we study these singularities numerically for general cases.

The organization of this paper is as follows. In Section 2, we formulate the crystalline curvature flow. In Section 3, we show some examples of degenerate pinching and discuss the singularities theoretically. In Section 4, we explain the numerical algorithm to estimate the extinction rate and show a numerical conjecture.

### §2. Crystalline curvature flow

Let  $f(\mathbf{n})$  be an interfacial energy defined on the unit circle  $S^1 = \mathbb{R}/2\pi\mathbb{Z}$ . First we consider the smooth case. The gradient flow of total interfacial energy on a simple closed curve  $\mathcal{P}$ ,  $\int_{\mathcal{P}} f(\mathbf{n}) ds$ , yields a weighted curvature flow  $V = (\sigma + \sigma'')K$ . Here  $ds$  is an arc-length parameter,  $V$  is a velocity in the  $\mathbf{n}$  direction,  $K$  is a curvature in the  $\mathbf{n}$  direction ( $K \equiv 1$  if  $\mathcal{P}$  is a unit circle), and  $\sigma(\theta) = f(\mathbf{n})$  ( $\theta$  is a normal angle which satisfies  $\mathbf{n} = -(\cos \theta, \sin \theta)$ ). We denoted  $\sigma'' = d^2\sigma/d\theta^2$ . When  $\sigma \equiv 1$ , this flow is well-known curve-shortening flow.

If the Wulff shape of  $\sigma$ , defined by

$$\mathcal{W}_\sigma = \bigcap_{\theta \in S^1} \{(x, y) \in \mathbb{R}^2 \mid x \cos \theta + y \sin \theta \leq \sigma(\theta)\}$$

is a convex polygon, then  $\sigma$  is not differentiable and the weighted curvature flow  $v = (\sigma + \sigma'')K$  is not well-defined in the usual sense. In

this case,  $f = \sigma$  is called *crystalline energy*. When  $\mathcal{W}_\sigma$  is an  $N_\sigma$ -sided polygon ( $N_\sigma \geq 3$ ), the set of its normal angles is defined as

$$\Phi_{N_\sigma} = \{\varphi_0, \varphi_1, \dots, \varphi_{N_\sigma-1}\},$$

where  $\varphi_n \in S^1$  is a normal angle of the  $n$ -th edge satisfying  $\varphi_0 < \varphi_1 < \dots < \varphi_{N_\sigma-1} < \varphi_0 + 2\pi$  with  $\varphi_{n+1} - \varphi_n < \pi$  for all  $n$  ( $\varphi_{N_\sigma} = \varphi_0 \bmod 2\pi$ ). Then the Wulff polygon  $\mathcal{W}_\sigma$  can be restated as follows:

$$\mathcal{W}_\sigma = \bigcap_{\varphi \in \Phi_{N_\sigma}} \{(x, y) \in \mathbb{R}^2 \mid x \cos \varphi + y \sin \varphi \leq \sigma(\varphi)\}.$$

When  $\sigma$  is a crystalline, we restrict curves to piecewise linear curves in a specific class in the following way: A curve  $\mathcal{P}$  has  $N$  vertices  $(x_j, y_j)$  ( $j = 0, 1, \dots, N - 1$ ), which are labeled in an anticlockwise order with  $(x_N, y_N) = (x_0, y_0)$ . Let  $\mathcal{S}_j = \{(1 - t)(x_j, y_j) + t(x_{j+1}, y_{j+1}) \mid 0 \leq t \leq 1\}$  be the  $j$ -th edge of  $\mathcal{P}$ . Then we may express  $\mathcal{P}$  as  $\mathcal{P} = \bigcup_{j=0}^{N-1} \mathcal{S}_j$ . Let  $\theta_j$  be a normal angle of  $\mathcal{S}_j$ . We say that  $\mathcal{P}$  is an  *$N$ -admissible curve* if the all normal angles belong to  $\Phi_{N_\sigma}$  and the angles of adjacent edges in  $\mathcal{P}$  are adjacent in  $\Phi_{N_\sigma}$  ( $\theta_N = \theta_0 \bmod 2\pi$ ).

For an admissible curve  $\mathcal{P}$ , the total interfacial crystalline energy is given by  $\sum_{j=0}^{N-1} \sigma(\theta_j) d_j$  ( $d_j$  is the length of  $\mathcal{S}_j$ ), and then the gradient flow (in the family of admissible curves) of this yields  $V_j = \chi_j l_\sigma(\theta_j) / d_j$ , where  $V_j$  is a normal velocity at  $\mathcal{S}_j$  in the inward normal direction  $\mathbf{n}_j = -(\cos \theta_j, \sin \theta_j)$ ,  $l_\sigma(\theta_j)$  is a length of the  $n$ -th edge of  $\mathcal{W}_\sigma$  satisfying  $\varphi_n = \theta_j$ , and  $\chi_j$  is a transition number, which takes  $+1$  (resp.  $-1$ ) if  $\mathcal{P}$  is convex (resp. concave) at  $\mathcal{S}_j$  in the  $\mathbf{n}_j$  direction; otherwise we set  $\chi_j = 0$ . The quantity

$$H_j = \chi_j \frac{l_\sigma(\theta_j)}{d_j}$$

is called *crystalline curvature*, and then  $V_j = H_j$  is called *crystalline curvature flow*. Note that  $\chi_j \equiv +1$  for all  $j$  if  $\mathcal{P}$  is a convex polygon, and that the every crystalline curvature of  $\mathcal{W}_\sigma$  equals  $+1$  on each edge.

In this paper we consider the following generalized crystalline curvature flow

$$(2) \quad V_j = a(\theta_j) \text{sign}(H_j) |H_j|^\alpha \quad \text{on } \mathcal{S}_j,$$

for  $j = 0, 1, \dots, N - 1$ , where  $\alpha$  is a positive parameter and  $a(\cdot)$  is a positive function which describes anisotropy of mobility.

Under the generalized crystalline curvature flow, each edge  $\mathcal{S}_j$  keeps the same normal angle but moves in the  $\mathbf{n}_j$  direction with the velocity

$v_j$ . Then we have the following system of ordinary differential equations

$$\dot{d}_j(t) = (\cot \vartheta_j + \cot \vartheta_{j-1})V_j - (\sin \vartheta_{j-1})^{-1}V_{j-1} - (\sin \vartheta_j)^{-1}V_{j+1}$$

for  $j = 0, 1, \dots, N - 1$  where  $\vartheta_j = \theta_{j+1} - \theta_j$ . Here and hereafter we denote  $(\dot{\cdot}) = d(\cdot)/dt$ . See, e.g., M.E. Gurtin [7]. The local existence and uniqueness of solutions of this problem follow from a general theory of system of ODEs. Therefore, if the initial curve  $\mathcal{P}(0)$  is admissible, then the admissibility of a solution curve  $\mathcal{P}(t)$  is preserved as long as all edges of the solution curve exist.

### §3. Examples of degenerate pinching singularities in nonconvex case

In this section, we show some examples for degenerate pinching singularities for nonconvex curves and discuss them theoretically. Throughout this section, we assume that the Wulff shape is a square ( $N_\sigma = 4$ ), centered at the origin, with  $\varphi_n = \pi n/2$  and  $l_\sigma(\varphi_n) \equiv 1$  for  $n = 0, 1, 2, 3$ . For more general case, we treat them numerically.

We first mention an example of a “capital L”-shaped (L-shaped in short) degenerate pinching singularity has been shown in [12].

**Example 1 (L-shaped).** Let the initial curve  $\mathcal{P}(0)$  be a 6-admissible elbow-like curve with  $\theta_j = \varphi_j$  ( $j = 0, 1, 2, 3$ ) and  $\theta_j = \varphi_{j-4}$  ( $j = 4, 5$ ). We assume symmetry of  $\mathcal{P}(0)$  such as  $d_0(0) = d_5(0)$ ,  $d_1(0) = d_4(0)$  and  $d_2(0) = d_3(0) = d_0(0) + d_1(0)$ . See Fig.3 (left) and Fig.4 (left). Suppose that  $\alpha \in (0, 1)$ , and that  $a(\varphi_n) = \mu \in (0, 1)$  for  $n = 0, 1$  and  $a(\varphi_n) = 1$  for  $n = 2, 3$ . If  $d_2(0)/d_1(0) \geq \max\{r_* + \varepsilon, (1 - \mu)^{-1/\alpha}\}$  for any fixed  $\varepsilon > 0$ , where  $r_* > 1$  satisfies  $r_*^{1-\alpha} - r_*^{-\alpha} - \mu = 0$ , then there exists  $T > 0$  such that  $\lim_{t \rightarrow T} d_1(t) = 0$  and  $\inf_{0 < t < T} d_2(t) > 0$  hold, that is, the nonconvex solution curve shrinks to an L-shaped line (see Fig.4). The extinction rate of  $d_1(t)$  is exactly  $T - t$ . (This is the same rate in the case of degenerate pinching singularity for convex curves.) We refer the reader [12, §3] for the proof, and [12, the second Remark in §3] and [14] for self-similar solutions of elbow-like curve (see also Fig.2).

Next we show “whisker”-type singularities.

**Example 2 (T-shaped).** Let the initial curve  $\mathcal{P}(0)$  be an 8-admissible “capital T”-shaped (T-shaped in short) curve with  $\theta_j = \varphi_j$  ( $j = 0, 1, 2, 3$ ) and  $\theta_4 = \varphi_2$ ,  $\theta_6 = \varphi_0$ ,  $\theta_5 = \theta_7 = \varphi_3$ . We assume  $d_0(0) = d_2(0)$ ,  $d_1(0) = d_3(0) + d_5(0) + d_7(0)$  and  $d_4(0) = d_6(0)$ . See Fig.3 (middle left). Suppose that  $\alpha \in (0, 1)$ , and that  $a(\varphi_n) = 1$  for  $n = 0, 1, 2$  and  $a(\varphi_3) = \mu > 0$ . If  $\mu \in (0, \mu')$  with  $\mu' = (d_4(0)/d_0(0))(d_5(0)/d_1(0))^\alpha$ ,

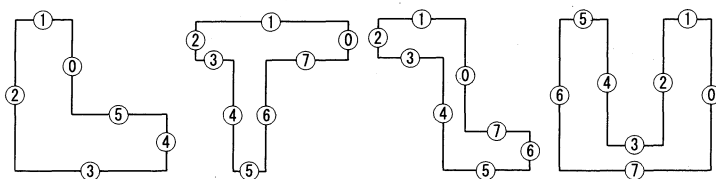


Fig. 3. Symmetric 6-admissible elbow-like curve (left), non-symmetric 8-admissible “capital T”-shaped curve (middle left), symmetric 8-admissible “capital Z”-shaped curve (middle right), and symmetric 8-admissible “capital U”-shaped curve (right). In each figure, the number  $i = 0, 1, \dots$  in a circle denotes the  $i$ -th edge.

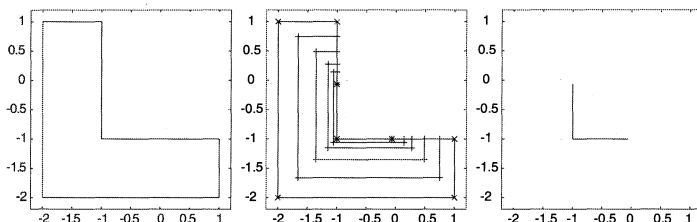


Fig. 4. Numerical simulations of L-shaped degenerate pinching singularity (case  $\alpha = 1/2$  and  $a(\varphi_n) \neq 1$ ). The initial symmetric 6-admissible elbow-like curve (left), time evolution of solution curves (middle) and the limit shape at  $t = T$  (right).

and  $C_0 = d_1(0)^{1-\alpha} - 2d_0(0)^{1-\alpha} > 0$  and  $d_i(0) > C_1$  for  $i = 3, 7$  with  $C_1 = (d_1(0) - C_0^{1/(1-\alpha)})/2 > 0$ , then there exists  $T > 0$  such that  $\lim_{t \rightarrow T} d_j(t) = 0$  ( $j = 0, 2$ ) and  $\inf_{0 < t < T} d_j(t) > 0$  ( $j \neq 0, 2$ ) hold, that is, the nonconvex solution curve shrinks to a rectangle with two whiskers. (See Fig.5). Moreover, the extinction rate of  $d_j(t)$  ( $j = 0, 2$ ) is exactly  $T - t$ .

*Proof.* From assumption, we have the following evolution equations:

$$\begin{aligned} \dot{d}_0 &= \dot{d}_2 = -d_1^{-\alpha}, & \dot{d}_1 &= -d_0^{-\alpha} - d_2^{-\alpha}, & \dot{d}_3 &= -d_2^{-\alpha}, \\ \dot{d}_4 &= \dot{d}_6 = -\mu d_5^{-\alpha}, & \dot{d}_5 &= 0, & \dot{d}_7 &= -d_0^{-\alpha}, \end{aligned}$$

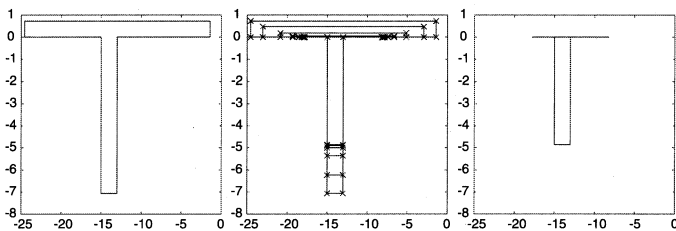


Fig. 5. Numerical simulation of T-shaped degenerate pinching singularity (case  $\alpha = 1/2$  and  $a(\varphi_n) \equiv 1$ ). The initial non-symmetric 8-admissible T-shaped curve (left), time evolution of solution curves (middle) and the limit shape at  $t = T$  (right).

since  $V_j = a(\theta_j)\chi_j d_j^{-\alpha}$ . Therefore we have

$$(3) \quad \dot{d}_0 = -d_1^{-\alpha}, \quad \dot{d}_1 = 2\dot{d}_3 = 2\dot{d}_7 = -2d_0^{-\alpha},$$

and also we have  $d_2(t) = d_0(t)$ ,  $d_5(t) = d_5(0)$ , and

$$(4) \quad d_4(t) = d_6(t) = d_4(0) - \frac{\mu}{d_5(0)^\alpha} t.$$

It holds that, by (3),

$$d_1(t)^{1-\alpha} = 2d_0(t)^{1-\alpha} + C_0, \quad C_0 = d_1(0)^{1-\alpha} - 2d_0(0)^{1-\alpha}.$$

Hence if  $C_0 > 0$ , then  $\inf_{t>0} d_1(t) > 0$  holds. Moreover, we have

$$(5) \quad \dot{d}_0 = -d_1^{-\alpha} = -(2d_0(t)^{1-\alpha} + C_0)^{-\alpha/(1-\alpha)}.$$

Therefore the maximal existence time of  $d_0(t)$  is less than or equal to  $T_1$ :

$$\begin{aligned} t &= \int_{d_0(t)}^{d_0(0)} (2\xi^{1-\alpha} + C_0)^{\alpha/(1-\alpha)} d\xi \\ &\leq \int_0^{d_0(0)} (2d_0(0)^{1-\alpha} + C_0)^{\alpha/(1-\alpha)} d\xi = d_0(0)d_1(0)^\alpha =: T_1. \end{aligned}$$

From (3)(right), for  $i = 3, 7$  we have

$$\begin{aligned} d_i(t) &= \frac{1}{2}((2d_0(t)^{1-\alpha} + C_0)^{1/(1-\alpha)} + 2d_i(0) - d_1(0)) \geq d_i(0) - C_1, \\ C_1 &= \frac{1}{2}(d_1(0) - C_0^{1/(1-\alpha)}) > 0. \end{aligned}$$

Hence if  $d_i(0) > C_1$ , then  $\inf_{t>0} d_i(t) > 0$  for  $i = 3, 7$ . On the other hand, from (4),  $d_4(t) = d_6(t) = 0$  holds just at  $t = T_2 = d_4(0)d_5(0)^\alpha/\mu$ . Therefore, if  $T_2 > T_1$ , then the first assertion holds. From (5),  $-c_1 < \dot{d}_0 < -c_2$  holds for some positive constants  $c_1$  and  $c_2$  since  $d_1$  is positive. By integration from  $t$  to  $T_1$ , we have the second assertion. Q.E.D.

**Example 3 (Z-shaped).** Let the initial curve  $\mathcal{P}(0)$  be an 8-admissible “capital Z”-shaped (Z-shaped in short) curve with  $\theta_j = \varphi_j$  ( $j = 0, 1, 2, 3$ ),  $\theta_j = \varphi_{j-2}$  ( $j = 4, 5$ ) and  $\theta_j = \varphi_{j-6}$  ( $j = 6, 7$ ). Put  $w_0 = d_0(0) - d_2(0) > -d_2(0)$ . We assume  $d_j(0) = d_{j+4}(0)$  ( $j = 0, 1, 2, 3$ ) and  $w_1 = d_1(0) - d_3(0) > 0$ . See Fig.3 (middle right) and Fig.6 (left). Suppose that  $\alpha \in (0, 1)$ , and that  $a(\varphi_n) = 1$  for  $n = 0, 2$  and  $a(\varphi_n) = \mu > 0$  for  $n = 1, 3$ . If  $w_0 > 0$  and  $\mu > \mu'$  with  $\mu' = d_2(0)^{1-\alpha}/(d_1(0)^{1-\alpha} - w_1^{1-\alpha})$ , then there exists  $T > 0$  such that  $\lim_{t \rightarrow T} d_j(t) = 0$  ( $j = 2, 6$ ) and  $\inf_{0 < t < T} d_j(t) > 0$  ( $j \neq 2, 6$ ) hold, that is, the nonconvex solution curve shrinks to a rectangle with two whiskers and the extinction rate of  $d_j(t)$  ( $j = 0, 2$ ) is exactly  $T - t$ . (See Fig.6). Moreover, if  $w_0 = 0$  and  $\mu > \mu'$ , then there exists  $T > 0$  such that  $\lim_{t \rightarrow T} d_j(t) = 0$  ( $j = 0, 2, 4, 6$ ) and  $\inf_{0 < t < T} d_j(t) > 0$  ( $j = 1, 3, 5, 7$ ) hold, that is, the nonconvex solution curve collapses to a line segment directly.

**Remark 3.1.** In case  $w_0 \in (-d_2(0), 0)$ , the nonconvex solution curve shrinks to a rectangle in a finite time, and eventually shrinks to a single point or a line segment.

*Proof.* From assumption, we have the following evolution equations:

$$\dot{d}_0 = \dot{d}_2 = -\mu d_1^{-\alpha}, \quad \dot{d}_1 = \dot{d}_3 = -d_2^{-\alpha},$$

and  $d_j(t) = d_{j+4}(t)$  ( $j = 0, 1, 2, 3$ ), since  $V_j = a(\theta_j)\chi_j d_j^{-\alpha}$ . Therefore we have

$$(6) \quad \dot{d}_1 = -d_2^{-\alpha}, \quad \dot{d}_2 = -\mu d_1^{-\alpha},$$

and  $d_0(t) - d_2(t) = w_0$  and  $d_1(t) - d_3(t) = w_1$  hold for  $t \geq 0$ . We note that there are no self-similar solutions since  $d_1(t) \geq w_1 > 0$ , and that there exists  $T > 0$  such that either  $\lim_{t \rightarrow T} d_2(t) = 0$  or  $\lim_{t \rightarrow T} d_3(t) = 0$  hold.

From (6),  $\mu \dot{d}_1/d_1^\alpha = \dot{d}_2/d_2^\alpha$ , and then

$$d_1(t)^{1-\alpha} = d_1(0)^{1-\alpha} - \frac{d_2(0)^{1-\alpha}}{\mu} + \frac{d_2(t)^{1-\alpha}}{\mu}.$$

By virtue of  $d_1(t) = d_3(t) + w_1$  and  $d_2(t)^{1-\alpha}/\mu \geq 0$ , it holds that

$$d_3(t) \geq \left( d_1(0)^{1-\alpha} - \frac{d_2(0)^{1-\alpha}}{\mu} \right)^{1/(1-\alpha)} - w_1,$$



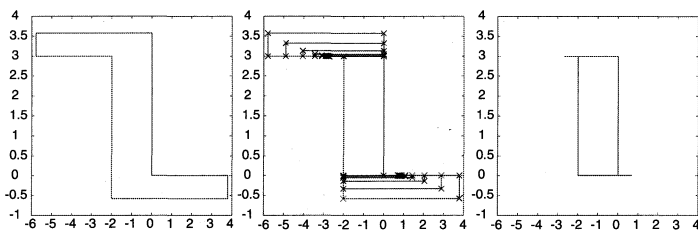


Fig. 6. Numerical simulation of Z-shaped degenerate pinching singularity (case  $\alpha = 1/2$  and  $a(\varphi_n) \equiv 1$ ). The initial symmetric 8-admissible Z-shaped curve (left), Time evolution of solution curves (middle) and the limit shape at  $t = T$  (right).

since  $\alpha < 1$ . Hence if  $\mu > \mu'$ , then the right hand side is positive, that is,  $\inf_{t>0} d_3(t) > 0$  holds, while there exists  $T > 0$  such that  $\lim_{t \rightarrow T} d_2(t) = 0$  holds, and so  $\lim_{t \rightarrow T} d_0(t) = w_0 \geq 0$  holds.

By the same argument in the previous example, we can obtain that the extinction rate of  $d_2(t)$  and  $d_6(t)$  is exactly  $T - t$ . Q.E.D.

**Example 4 (U-shaped).** Let the initial curve  $\mathcal{P}(0)$  be an 8-admissible “capital U”-shaped (U-shaped in short) curve with  $\theta_j = \varphi_j$  ( $j = 0, 1, 2$ ),  $\theta_3 = \varphi_1$  and  $\theta_j = \varphi_{j-4}$  ( $j = 4, 5, 6, 7$ ). Put  $u = d_1(0)/d_3(0)$ ,  $v = d_1(0)/d_0(0)$  and  $w = (d_0(0) - d_2(0))/d_0(0)$ . We assume  $d_{3+i}(0) = d_{3-i}(0)$  ( $i = 1, 2, 3$ ),  $d_7(0) = d_3(0) + 2d_1(0)$  and  $w \in (0, 1)$ . See Fig.3 (right). Suppose that  $\alpha \in (0, 1)$ , and that  $a(\varphi_n) = \mu > 0$  for  $n = 0, 2$ ,  $a(\varphi_1) = \lambda > 0$  and  $a(\varphi_3) = \rho > 0$ . Put

$$d_{02}(t) = d_0(t) - d_2(t).$$

Then there exists a time  $T > 0$  such that at least one of  $d_1(t)$ ,  $d_2(t)$  or  $d_{02}(t)$  converges to zero as  $t$  tends to  $T$ , and  $d_j(t) > 0$  holds for  $t \in [0, T)$ ,  $j = 1, 2, 02$ . Therefore five limit shapes are possible as in Table 1.

The case (a) is similar to the previous two examples. The case (b) means that the region enclosed by solution curve is split. The other cases are a combination or special case of (a) and (b). In the following, we will consider only cases (a) and (b). (See Fig.7).

From assumption, we have the following evolution equations:

$$\dot{d}_0 = -\lambda d_1^{-\alpha} - \rho d_7^{-\alpha}, \quad \dot{d}_1 = -\mu d_0^{-\alpha}, \quad \dot{d}_2 = -\lambda d_1^{-\alpha} - \lambda d_3^{-\alpha}, \quad \dot{d}_3 = 0,$$

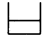



as $t \rightarrow T$	(a)	(b)	(c)	(d)	(e)
				—	
$d_1(t)$	0	+	0	+/0	+/0
$d_2(t)$	+	+	+	0	0
$d_{02}(t)$	+	0	0	0	+

Table 1. Possible five limit shapes at a time  $T$  in the U-shaped case. In the table, the mark “+” means  $\inf_{0 < t < T} d_j(t) > 0$ , and “0” means  $\lim_{t \rightarrow T} d_j(t) = 0$  for  $j = 1, 2$  and  $02$ .

and  $d_{3+i}(t) = d_{3-i}(t)$  ( $i = 1, 2, 3$ ), since  $V_j = a(\theta_j)\chi_j d_j^{-\alpha}$ . Therefore we have

$$\begin{aligned}
 (7) \quad & \dot{d}_0 = -\lambda d_1(t)^{-\alpha} - \rho(d_3(0) + 2d_1(t))^{-\alpha}, \\
 (8) \quad & \dot{d}_1 = -\mu d_0(t)^{-\alpha}, \\
 (9) \quad & \dot{d}_2 = -\lambda d_1(t)^{-\alpha} - \lambda d_3(0)^{-\alpha}, \\
 (10) \quad & \dot{d}_{02} = \lambda d_3(0)^{-\alpha} - \rho(d_3(0) + 2d_1(t))^{-\alpha}.
 \end{aligned}$$

We note that there are no self-similar solutions since  $d_3(t) = d_3(0) > 0$ .

**Case (a).** From (7),  $d_1(0) \geq d_1(t)$ , and  $d_3(0) + 2d_1(t) \geq d_1(t)/u + 2d_1(t) = (2 + u^{-1})d_1(t)$ , we have

$$\dot{d}_0 \geq -\left(\lambda + \frac{\rho}{(2 + u^{-1})^\alpha}\right) d_1^{-\alpha}.$$

Then by (8),

$$d_0^{-\alpha} \dot{d}_0 \geq -\left(\lambda + \frac{\rho}{(2 + u^{-1})^\alpha}\right) d_0^{-\alpha} d_1^{-\alpha} = \frac{M_0}{\mu} d_1^{-\alpha} \dot{d}_1.$$

Here

$$M_0 = \lambda + \frac{\rho}{(2 + u^{-1})^\alpha}.$$

By the assumption  $\alpha \in (0, 1)$ ,  $(d_0^{1-\alpha})' \geq M_0(d_1^{1-\alpha})'/\mu$  holds, and then we obtain

$$d_0(t)^{1-\alpha} \geq d_0(0)^{1-\alpha} - \frac{M_0}{\mu} d_1(0)^{1-\alpha} = d_0(0)^{1-\alpha} \left(1 - \frac{M_0}{\mu} v^{1-\alpha}\right),$$

since  $d_1(t)^{1-\alpha} \geq 0$ .

Hence if we assume

$$(A0) \quad \mu > M_0 v^{1-\alpha},$$

then we have the positivity of  $d_0(t)$  for all  $t$ :

$$d_0(t) \geq C_0, \quad C_0 = d_0(0) \left( 1 - \frac{M_0}{\mu} v^{1-\alpha} \right)^{1/(1-\alpha)} > 0.$$

By (10) and  $d_1(0) \geq d_1(t)$ , we have

$$\dot{d}_{02}(t) \leq \frac{\lambda}{d_3(0)^\alpha} - \frac{\rho}{d_3(0)^\alpha(1+2u)^\alpha} = - \left( \frac{u}{vd_0(0)} \right)^\alpha \left( \frac{\rho}{(1+2u)^\alpha - \lambda} \right).$$

Therefore if we assume

$$(A1) \quad \frac{\lambda(1+2u)^\alpha}{\rho} < 1,$$

then

$$C_1 = \left( \frac{u}{vd_0(0)} \right)^\alpha \left( \frac{\rho}{(1+2u)^\alpha - \lambda} \right) > 0$$

holds, and we have  $\dot{d}_{02}(t) \leq -C_1$ .

Assume (A0) and (A1), then  $d_{02}(t) \leq d_{02}(0) - C_1 t = wd_0(0) - C_1 t$  holds, and so we have

$$d_2(t) \geq C_0 - wd_0(0) = d_0(0) \left( \left( 1 - \frac{M_0}{\mu} v^{1-\alpha} \right)^{1/(1-\alpha)} - w \right).$$

Hence if we assume (A1) and

$$(A2) \quad \mu > \mu_{\text{inf}}, \quad \mu_{\text{inf}} = \frac{M_0}{1 - w^{1-\alpha}} v^{1-\alpha},$$

then we have the positivity of  $d_2(t)$  for all  $t$ :

$$d_2(t) \geq C_2, \quad C_2 = C_0 - wd_0(0) > 0,$$

since if (A2), then (A0) holds.

If we assume (A0), then by  $d_2(t) \leq d_2(0) = (1-w)d_0(0)$  we have

$$d_{02}(t) \geq C_0 - (1-w)d_0(0) = d_0(0) \left( \left( 1 - \frac{M_0}{\mu} v^{1-\alpha} \right)^{1/(1-\alpha)} - 1 + w \right).$$

Hence if we assume

$$(A3) \quad \mu > \mu'_{\text{inf}}, \quad \mu'_{\text{inf}} = \frac{M_0}{1 - (1 - w)^{1-\alpha}} v^{1-\alpha},$$

then we have the positivity of  $d_{02}(t)$  for all  $t$ :

$$d_{02}(t) \geq C_4, \quad C_4 = C_0 - (1 - w)d_0(0) > 0,$$

since if (A3), then (A0) holds.

Q.E.D.

Consequently, we have the following assertion:

**Lemma 3.2** (Case (a)). *Assume (A1), (A2) and (A3), then there exists  $T > 0$  such that  $\inf_{0 < t < T} d_j(t) > 0$  holds for  $j = 2, 02$ , and  $\lim_{t \rightarrow T} d_1(t) = 0$  holds.*

**Remark 3.3.** The set of parameters  $\{\alpha \in (0, 1), \mu, \lambda, \rho > 0\}$  satisfying (A1), (A2) and (A3) is not empty for any parameters of the initial shape  $\{u, v > 0, w \in (0, 1)\}$ . Conversely, for any  $\alpha \in (0, 1)$ ,  $\mu > 0$  and  $\rho > \lambda > 0$ , one can find  $u$  satisfying (A1), and  $v$  and  $w$  satisfying (A2) and (A3), since small  $\mu_{\text{inf}}$  and  $\mu'_{\text{inf}}$  can be achieved taking small  $v > 0$ . In Fig.7, Case (a), we show a numerical example using the parameters satisfying all of the assumptions: The parameters are  $\alpha = 1/2, \mu = 27, \lambda = 0.1, \rho = 16$ , and the data of the initial shape are  $d_0(0) = d_6(0) = 8, d_1(0) = 1, d_2(0) = 7, d_3(0) = 9, d_7(0) = 11$ . Note that assumptions (A1), (A2) and (A3) are sufficient conditions. One can control parameters which realize case (a), at least numerically, without satisfying some of the assumptions. Fig.8 (a) (upper middle) suggests that such parameters exist: All the parameters except  $\alpha = 2/3$  are the same as those in the above example of Fig.7, Case (a).

**Case (b).** From (8), (9) and  $-\dot{d}_2 \geq \lambda d_1^{-\alpha}$ , we have

$$\ddot{d}_2 = \frac{\alpha \lambda}{d_1^{1+\alpha}} \dot{d}_1 = -\frac{\alpha \lambda \mu}{d_0^\alpha d_1^{1+\alpha}} \geq -\frac{\alpha \lambda \mu}{d_0^\alpha} \left( \frac{-\dot{d}_2}{\lambda} \right)^{(1+\alpha)/\alpha}.$$

If we assume (A0), then

$$\ddot{d}_2 \geq -\frac{\alpha \mu}{C_0^\alpha \lambda^{1/\alpha}} (-\dot{d}_2)^{(1+\alpha)/\alpha}.$$

We put  $D_2 = -\dot{d}_2$ , and we obtain

$$-\left( D_2^{-1/\alpha} \right)' \leq \frac{\mu}{C_0^\alpha \lambda^{1/\alpha}}.$$

Integration of this over  $(0, t)$  yields

$$(11) \quad D_2(t)^{-1/\alpha} \geq D_2(0)^{-1/\alpha} - \frac{\mu}{C_0^\alpha \lambda^{1/\alpha}} t.$$

By (9), we have

$$D_2(0)^{-1/\alpha} = \left(-\dot{d}_2(0)\right)^{-1/\alpha} = \frac{vd_0(0)}{\lambda^{1/\alpha}(1+u^\alpha)^{1/\alpha}}.$$

By the way, from (10) and  $d_1(t) \leq d_1(0)$ , we have  $\dot{d}_{02} \leq -C_1$ , and so  $d_{02}(t) \leq wd_0(0) - C_1 t$  holds. Hence if we assume (A1), then  $C_1 > 0$  and the maximum existence time of  $d_{02}(t)$  is less than or equal to  $T_{02}$ :

$$T_{02} = \frac{wd_0(0)}{C_1}.$$

Hereafter we will show that  $d_1(t)$  is positive at least until  $t = T_{02}$ . From (11), we have

$$D_2(t)^{-1/\alpha} \geq C_5, \quad C_5 = D_2(0)^{-1/\alpha} - \frac{\mu}{C_0^\alpha \lambda^{1/\alpha}} T_{02}.$$

Therefore if  $C_5 > 0$ , then

$$D_2(t) = -\dot{d}_2 = \lambda d_1^{-\alpha} + \lambda d_3(0)^{-\alpha} \leq C_5^{-\alpha},$$

and so  $d_1^{-\alpha} \leq (C_5^{-\alpha} - \lambda d_3(0)^{-\alpha})/\lambda$  holds. Here we claim that  $C_5^{-\alpha} > \lambda d_3(0)^{-\alpha}$  holds. Indeed, we have

$$0 < C_5 < D_2(0)^{-1/\alpha} = \frac{1}{\lambda^{1/\alpha}} \left(\frac{u^\alpha}{1+u^\alpha}\right)^{1/\alpha} d_3(0) < \frac{d_3(0)}{\lambda^{1/\alpha}}.$$

Hence if  $C_5 > 0$ , then we have

$$d_1(t) \geq C_6, \quad C_6 = \lambda^{1/\alpha}(C_5^{-\alpha} - \lambda d_3(0)^{-\alpha})^{-1/\alpha} > 0,$$

for all  $t \in [0, T_{02}]$ .

Now we will show  $C_5 > 0$ . If we assume (A1) and (A2), then  $d_2(t) \geq C_2 = C_0 - wd_0(0) > 0$  holds. Therefore we have

$$\begin{aligned} C_5 &= \frac{vd_0(0)}{\lambda^{1/\alpha}(1+u^\alpha)^{1/\alpha}} - \frac{w\mu d_0(0)^{1+\alpha}}{\lambda^{1/\alpha}(\rho - \lambda(1+2u)^\alpha)} \left(\frac{v(1+2u)}{C_0 u}\right)^\alpha \\ &> \frac{d_0(0)}{\lambda^{1/\alpha}} \left(\frac{v(1+2u)}{u}\right)^\alpha \left(M_1 v^{1-\alpha} - \frac{\mu w^{1-\alpha}}{\rho - \lambda(1+2u)^\alpha}\right). \end{aligned}$$

Here

$$M_1 = \frac{1}{(1 + u^\alpha)^{1/\alpha}} \left( \frac{u}{1 + 2u} \right)^\alpha.$$

If we assume

$$(A4) \quad \frac{M_1(\rho - \lambda(1 + 2u)^\alpha)}{w^{1-\alpha}} > \frac{M_0}{1 - w^{1-\alpha}},$$

then  $\mu_{\text{sup}} > \mu_{\text{inf}}$  holds, where

$$\mu_{\text{sup}} = \frac{M_1(\rho - \lambda(1 + 2u)^\alpha)}{w^{1-\alpha}} v^{1-\alpha}.$$

Hence we can assume (A2) and

$$(A5) \quad \mu_{\text{sup}} \geq \mu,$$

simultaneously, and then finally we obtain  $C_5 > 0$ .

Let  $T$  be an extinction time. Then, from positivity and boundedness of  $d_1$  and  $C_1 > 0$ , we have  $-C_7 < \dot{d}_{02} < -C_8$  for some positive constants  $C_7$  and  $C_8$ . Thus, the extinction rate of  $d_{02}(t)$  is exactly  $T - t$ . Q.E.D.

Consequently, we have the following assertion:

**Lemma 3.4** (Case (b)). *Assume (A1), (A2), (A4) and (A5), then there exists  $T > 0$  such that  $\inf_{0 < t < T} d_j(t) > 0$  holds for  $j = 1, 2$ , and  $\lim_{t \rightarrow T} d_{02}(t) = 0$  holds. Moreover, the extinction rate of  $d_{02}(t)$  is exactly  $T - t$ .*

**Remark 3.5.** Under the conditions  $\alpha \in (0, 1)$ ,  $w \in (0, 1)$  and (A1), the assumption (A4) is equivalent to the following inequality

$$\rho(1 - \delta) \left( \frac{u}{1 + 2u} \right)^\alpha + \lambda(1 + \delta u^\alpha) < 0, \quad \delta = \frac{1 - w^{1-\alpha}}{w^{1-\alpha}} \frac{1}{(1 + u^\alpha)^{1/\alpha}}.$$

If  $\alpha \lesssim 1$  or  $w \lesssim 1$  or  $u$  is sufficiently large, then  $\delta < 1$  holds and the left hand side of the above inequality is positive. Therefore (A4) is not satisfied. However, for parameters of the initial shape  $\{u, v > 0, w \in (0, 1)\}$  in an appropriate range, the set of parameters  $\{\alpha \in (0, 1), \mu, \lambda, \rho > 0\}$  satisfying (A1), (A2), (A4) and (A5) is not empty, and the converse is also true. In Fig.7, Case (b), we show a numerical example using the parameters satisfying all of the assumptions. The initial shape and all the parameters except  $\mu = 2.694$  are the same as those in Fig.7, Case (a) (see Remark 3.3). Note that assumptions (A1), (A2), (A4) and (A5) are sufficient conditions. One can control parameters which realize case (b), at least numerically, without satisfying some of the assumptions.

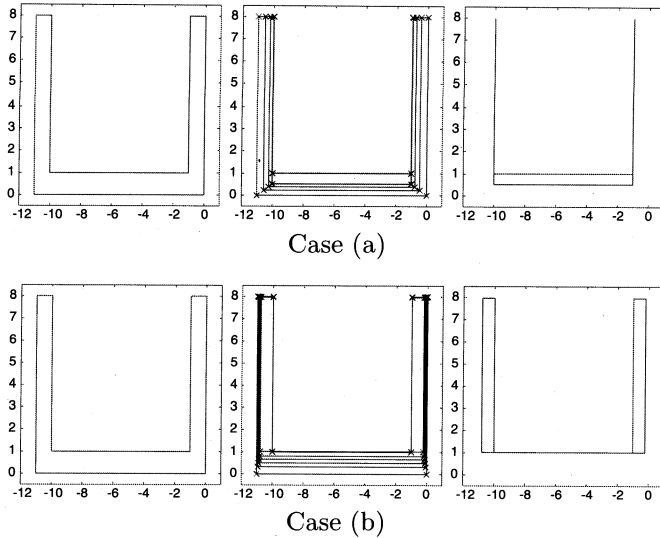


Fig. 7. Numerical simulation for U-shaped curves (case  $\alpha = 1/2$  and  $a(\varphi_n) \neq 1$ ). The upper figures show the time evolution of solution curves in the case (a). The lower figures are for the case (b): The initial symmetric 8-admissible U-shaped curve (left), time evolution of solution curves (middle) and the limit shape at  $t = T$  (right). See Remark 3.3 and 3.5 for the data and comments.

Fig.8 (b) (upper right) suggests that such parameters exist: All the parameters except  $\alpha = 1/3$  and  $\mu = 3$  are the same as those in the above example of Fig.7, Case (b).

**Remark 3.6.** In Fig.8, we show examples which realize all limit shapes numerically starting with the same initial shape and changing only the parameters. The initial shape is the same as one in Fig.7, Case (a) (see Remark 3.3), and the parameters are given in Table 2. Conversely, one can easily realize the limit shapes in the cases (a), (b) and (e) numerically controlling only the initial shapes without changing parameters, while we need fine tuning to realize the cases (c) and (d).

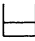


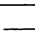

	$\alpha$	$\mu$	$\lambda$	$\rho$	(A1)	(A2)	(A3)	(A4)	(A5)
(a) 	2/3	27	0.1	16	OK.	OK.	/	/	/
(b) 	1/3	3	0.1	16	OK.	OK.	/	/	/
(c) 	1/2	13.8	0.1	16	OK.	OK.	/	OK.	/
(d) 	1/2	0.1	9.25	16	OK.	/	/	/	OK.
(e) 	1/2	27	50	16	/	/	/	/	/

Table 2. The parameters in Fig.8. See Remark 3.6.

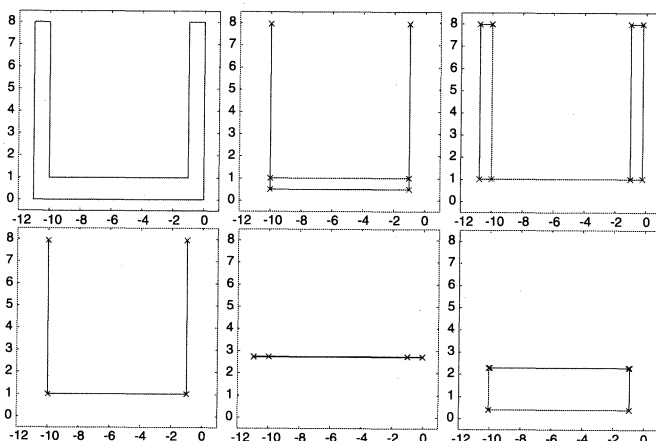


Fig. 8. Numerical examples of all limit shapes starting with the same initial shape (upper left). See Remark 3.6 in detail.

#### §4. Numerical algorithm and results

In [9, 10], Hirota and Ozawa developed a new numerical estimating method of blow-up time and  $(T - t)^{-p}$  type blow-up rate of solutions to a system of ordinary differential equations. We apply this method to  $1/d_j(t)$  and estimate  $(T - t)^{-p}$  type extinction rate numerically.

Let us consider the following system of ordinary differential equations:

$$\frac{d}{dt}y_j(t) = f_j(t, y_0, \dots, y_{N-1}), \quad j = 0, 1, \dots, N - 1.$$



We suppose that some of  $y_j(t)$  blow up in finite time  $T$ . The numerical method consists of the following three parts:

**Part 1. Arc-length transformation technique.** We translate the blow-up problem to the following:

$$\frac{d}{ds} \begin{pmatrix} t(s) \\ y_0(s) \\ \vdots \\ y_{N-1}(s) \end{pmatrix} = \frac{1}{\sqrt{1 + \sum_{k=0}^{N-1} f_k^2}} \begin{pmatrix} 1 \\ f_0 \\ \vdots \\ f_{N-1} \end{pmatrix}, \quad t(0) = 0.$$

From this transformation, a solution of a new system never blows up in a finite time even if the solution of the original problem blows up in a finite time. This transformation is called *arc-length transformation*.

**Part 2. Generate a linearly convergent sequence to  $T$ .** Assume that there is only  $(T - t)^{-p}$  type singularity. Here  $p > 0$ , and  $T$  is a blow-up time of the original problem. We note that blow-up time is given by

$$T = \int_0^\infty \frac{ds}{\sqrt{1 + \sum_{k=0}^{N-1} f_k^2}}.$$

Let  $\{s_n\}$  be the geometric sequence given by

$$s_n = s_0 r^n \quad (s_0 > 0, r > 1, n = 0, 1, 2, \dots),$$

and let  $\{t_n\}$  be the time sequence given by

$$t_n = \int_0^{s_n} \frac{ds}{\sqrt{1 + \sum_{k=0}^{N-1} f_k^2}}.$$

Then  $\{t_n\}$  converges to  $T$  linearly, that is,  $\lim_{n \rightarrow \infty} |e_n/e_{n-1}| = r^{-1/p}$ , where  $e_n = T - t_n$ .

**Part 3. Acceleration by the Aitken  $\Delta^2$  method.** The Aitken  $\Delta^2$  method can be applied to linearly convergent sequence in order to accelerate the convergence. Thus, we obtain an *approximation of the blow-up time*, say  $\tilde{T}$ . Using  $\tilde{T}$  instead of  $T$ , we can calculate an approximate value of  $p$  by  $p \simeq p_n = -\log r / \log |\tilde{e}_n/\tilde{e}_{n-1}|$ , where  $\tilde{e}_n = \tilde{T} - t_n$ . From this procedure, we obtain a sequence  $\{p_n\}$  and extinction rate numerically. For a numerical integrator of ODEs from  $s = s_{n-1}$  to  $s = s_n$ , we use the DOPRI5 code (see [8]) with parameters ITOL=0 and RTOL=ATOL=1.d-15 and we set  $s_n = 1 \cdot 2^n$  ( $s_0 = 1$  and  $r = 2$ ). And

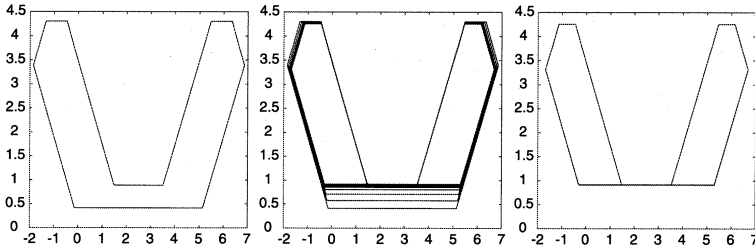


Fig. 9. Numerical simulation of splitting-type degenerate pinching singularity (case  $N_\sigma = 6$ ,  $\alpha = 1/2$  and  $a(\varphi_n) \neq 1$ ). The initial 10-admissible curve (left), time evolution of solution curves (middle) and the limit shape at  $t = T$  (right).

we apply the Aitken  $\Delta^2$  method three times. All computations are performed by using the double precision IEEE arithmetic.

Here we only treat splitting-type singularities. Note that the flows are not isotropic. In this case, we introduce a new variable  $w(t)$  which is the distance between two parallel edges which are touched each other at splitting time  $T$ . We consider the extinction rate of  $w(t) \sim (T - t)^p$ . Table 3 (a) shows the sequence  $\{p_n\}$  in the case where the Wulff shape is a regular hexagon centered at the origin ( $N_\sigma = 6$ ), and  $\alpha = 1/2$  and  $a(\varphi_n) \neq 1$ . Fig.9 (middle) shows time evolution of solution curves with the initial shape (left) and the limit shape at  $t = T$  (right). From them we see that the solution polygon splits two regions at  $t = T$  and the extinction rate is exactly  $T - t$  ( $p = 1$ ). Table 3 (b) shows the sequence  $\{p_n\}$  in the case where the Wulff shape is a regular octagon centered at the origin ( $N_\sigma = 8$ ), and  $\alpha = 1/2$  and  $a(\varphi_n) \neq 1$ . Fig.10 (middle) shows time evolution of solution curves with the initial shape (left) and the limit shape at  $t = T$  (right). From them we see that the solution polygon splits two regions at  $t = T$  and the extinction rate is exactly  $T - t$  ( $p = 1$ ).

From the above numerical computations and the examples in the previous section suggest that in every splitting-type degenerate pinching cases the extinction rate is exactly  $T - t$  or very close to  $T - t$ .

**Conjecture I.** *Suppose that  $0 < \alpha < 1$  and a solution polygon splits more than two regions and let  $w(t)$  be the width of the pinching part. Then there exist two positive constants  $c_1$  and  $c_2$  such that  $c_1(T - t)^{1+\epsilon} \leq w(t) \leq c_2(T - t)^{1-\epsilon}$  for any  $\epsilon > 0$ .*

$n$	$p_n$	$n$	$p_n$	$n$	$p_n$	$n$	$p_n$
1	1.818e+00	7	1.013e+00	1	1.472e+00	7	1.002e+00
2	1.404e+00	8	1.006e+00	2	1.157e+00	8	1.001e+00
3	1.202e+00	9	1.003e+00	3	1.053e+00	9	1.000e+00
4	1.101e+00	10	1.002e+00	4	1.019e+00	10	1.000e+00
5	1.051e+00	11	1.001e+00	5	1.008e+00	11	1.000e+00
6	1.025e+00	12	1.000e+00	6	1.004e+00	12	1.000e+00

(a)  $N_\sigma = 6$

(b)  $N_\sigma = 8$

Table 3. Convergent behavior of extinction rate.

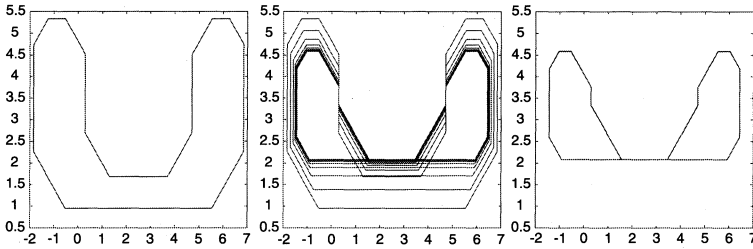


Fig. 10. Numerical simulation of splitting-type degenerate pinching singularity (case  $N_\sigma = 8$ ,  $\alpha = 1/2$  and  $a(\varphi_n) \neq 1$ ). The initial 16-admissible curve (left), time evolution of solution curves (middle) and the limit shape at  $t = T$  (right).

**Acknowledgements.** We would like to thank the referee for her or his comments and suggestions.

### References

- [ 1 ] F. Almgren and J. E. Taylor, Flat flow is motion by crystalline curvature for curves with crystalline energies, *J. Diff. Geom.*, **42** (1995), 1–22.
- [ 2 ] B. Andrews, Singularities in crystalline curvature flows, *Asian J. Math.*, **6** (2002), 101–122.
- [ 3 ] S. Angenent and M. E. Gurtin, Multiphase thermomechanics with interfacial structure, 2. Evolution of an isothermal interface, *Arch. Rational Mech. Anal.*, **108** (1989), 323–391.
- [ 4 ] K. S. Chou and X. P. Zhu, A convexity theorem for a class of anisotropic flows of plane curves, *Indiana Univ. Math. J.*, **48** (1999), 139–154.

- [ 5 ] M.-H. Giga and Y. Giga, Crystalline and level set flow – convergence of a crystalline algorithm for a general anisotropic curvature flow in the plane, In: Free boundary problems: theory and applications, I, Chiba, 1999, GAKUTO Internat. Ser. Math. Sci. Appli., **13**, Gakkōtoshō, Tokyo, 2000, pp. 64–79.
- [ 6 ] M. Grayson, The heat equation shrinks embedded plane curves to round points, *J. Diff. Geom.*, **26** (1986), 69–96.
- [ 7 ] M. E. Gurtin, Thermomechanics of evolving phase boundaries in the plane, Oxford, Clarendon Press, 1993.
- [ 8 ] E. Hairer, S. P. Nørsett and G. Wanner, Solving Ordinary Differential Equations I, 2nd rev. ed., Springer, Berlin, 2000; Fortran source of DOPRI5 is available at the web site <http://www.unige.ch/math/folks/hairer/software.html> .
- [ 9 ] C. Hirota and K. Ozawa, A method of estimating the blow-up time and blow-up rate of the solution of the system of ordinary differential equations —An application to the blow-up problems of partial differential equations—, *Transactions of the Japan Society for Industrial and Applied Mathematics*, **14** (2004), 13–38.
- [ 10 ] C. Hirota and K. Ozawa, Numerical method of estimating the blow-up time and rate of the solution of ordinary differential equations—an application to the blow-up problems of partial differential equations, *J. Comput. Appl. Math.*, **193** (2006), 614–637.
- [ 11 ] C. Hirota, T. Ishiwata and S. Yazaki, Some results on singularities of solutions to an anisotropic crystalline curvature flow. Mathematical approach to nonlinear phenomena: modelling, analysis and simulations, GAKUTO Internat. Ser. Math. Sci. Appl., **23**, Gakkōtoshō, Tokyo, 2005, pp. 119–128.
- [ 12 ] C. Hirota, T. Ishiwata and S. Yazaki, Note on the asymptotic behavior of solutions to an anisotropic crystalline curvature flow, In: Recent Advances on Elliptic and Parabolic Issues, Proceedings of the 2004 Swiss-Japan Seminar, (eds. Michel Chipot and Hirokazu Ninomiya), World Scientific, 2006, pp. 129–143.
- [ 13 ] K. Ishii and H. M. Soner, Regularity and convergence of crystalline motion, *SIAM J. Math. Anal.*, **30** (1999), 19–37 (electronic).
- [ 14 ] T. Ishiwata, T. K. Ushijima, H. Yagisita and S. Yazaki, Two examples of nonconvex self-similar solution curves for a crystalline curvature flow, *Proc. Japan Acad. Ser. A Math. Sci.*, **80** (2004), 151–154.
- [ 15 ] T. Ishiwata and S. Yazaki, On the blow-up rate for fast blow-up solutions arising in an anisotropic crystalline motion, *J. Comp. App. Math.*, **159** (2003), 55–64.
- [ 16 ] T. Ishiwata and S. Yazaki, A fast blow-up solution and degenerate pinching arising in an anisotropic crystalline motion, preprint.
- [ 17 ] A. Stancu, Asymptotic behavior of solutions to a crystalline flow, *Hokkaido Math. J.*, **27** (1998), 303–320.

- [18] J. E. Taylor, Constructions and conjectures in crystalline nondifferential geometry, In: Proceedings of the Conference on Differential Geometry, Rio de Janeiro, Pitman Monographs Surveys Pure Appl. Math., **52**, Pitman London, 1991, pp. 321–336.

Chiaki Hirota

*Faculty of Systems Science and Technology*

*Akita Prefectural University*

*84-4 Ebinokuchi, Tsuchiya, Akita 015-0055, Japan*

Tetsuya Ishiwata

*Faculty of Education*

*Gifu University*

*1-1 Yanagido, Gifu 501-1193, Japan*

Shigetoshi Yazaki

*Faculty of Engineering*

*University of Miyazaki*

*1-1 Gakuen Kibanadai Nishi, Miyazaki 889-2192, Japan*